# Determination of the creep function of viscoelastic pipelines using system resonant frequencies with hydraulic transient analysis

Jinzhe Gong[1], Aaron C. Zecchin[2], Martin F. Lambert[3] and Angus R. Simpson[4]

[1]Research Associate; School of Civil, Environmental and Mining Engineering, University of Adelaide, SA 5005, Australia; Email: jinzhe.gong@adelaide.edu.au

[2]Senior Lecturer; School of Civil, Environmental and Mining Engineering, University of Adelaide, SA 5005, Australia; Email: aaron.zecchin@adelaide.edu.au

[3]Professor; M.ASCE; School of Civil, Environmental and Mining Engineering, University of Adelaide, SA 5005, Australia; Email: martin.lambert@adelaide.edu.au

[4]Professor; M.ASCE; School of Civil, Environmental and Mining Engineering, University of Adelaide, SA 5005, Australia; Email: angus.simpson@adelaide.edu.au

**Abstract**

The determination of the creep (compliance) function of viscoelastic pipelines is essential for modelling their hydraulic behavior and accurately predicting pressure responses under transient events. This paper proposes a novel frequency-domain technique for the determination of the creep function of viscoelastic pipelines using hydraulic transients. A viscoelastic pipeline system, when compared with a frictionless elastic pipeline under the same system configuration, has non-uniformly shifted resonant frequencies. Analytical

analysis shows that the shift in the resonant frequencies of a viscoelastic pipeline system is related to both the pipe wall viscoelastic compliance effects and the unsteady wall shear stress effects. A technique is developed to determine the elastic wave speed and the viscoelastic creep compliances based on the shifted system resonant frequencies. To improve the accuracy of the calibration for the viscoelastic parameters, an approach is proposed to correct the shifting in the resonant frequencies induced by the unsteady friction before the calibration. Numerical simulations conducted on a high-density polyethylene (HDPE) pipeline verify that the elastic wave speed and viscoelastic compliance can be determined with relatively high accuracy.

*Keywords*: creep function; fluid transient; polymer; resonance; viscoelasticity; water hammer.

## Introduction

Viscoelastic pipelines, such as polyvinyl chloride (PVC) and high-density polyethylene (HDPE) pipelines, have been increasingly used throughout the world for potable water distribution, sewage effluent transport and agriculture irrigation. Experimental studies (Güney 1983; Covas et al. 2004; Ramos et al. 2004; Brunone and Berni 2010; Meniconi et al. 2012; Pezzinga et al. 2014) showed that transient pressure waves experienced greater attenuation and dispersion in viscoelastic pipelines when compared with elastic pipelines (e.g. metallic pipes). However, in some cases, the use of viscoelastic pipelines increases the maximum transient pressure (Pezzinga and Scandura 1995; Ramos et al. 2004). In the frequency domain, viscoelasticity introduces non-uniform (frequency-dependent) shifting

of the resonant frequencies of a pipeline system and non-uniform resonant responses (Suo and Wylie 1990; Lee et al. 2013). Detailed understanding of the hydraulic characteristics of viscoelastic pipelines is critical for accurate prediction of the pressure responses of a pipeline system during transient events, better system design and safe operation.

A number of studies, both in the time and the frequency domain, have been conducted and reported in the literature on the development of a mathematical model to describe the hydraulic transient response of viscoelastic pipelines. For an applied pressure load within a pipe (as experienced during a water hammer event), the effect of viscoelasticity is characterized by an instantaneous elastic strain, followed by a gradual retarded strain (Covas et al. 2004; Shaw and MacKnight 2005). In the time domain, the method of characteristics (MOC) (Wylie and Streeter 1993; Chaudhry 2014) was used and an additional viscoelastic term was added into the classic continuity equation to describe the retarded wall deformation (Gally et al. 1979; Rieutord and Blanchard 1979; Güney 1983; Pezzinga and Scandura 1995; Ramos et al. 2004; Covas et al. 2005; Soares et al. 2008; Meniconi et al. 2012; Meniconi et al. 2014). Within all this work, a linear viscoelastic mechanical model, the generalized Kelvin-Voigt (K-V) model (Shaw and MacKnight 2005) that includes an elastic element and one or more viscoelastic elements, was used to describe the retarded wall deformation by mathematically describing the creep function of a viscoelastic pipeline. The creep function, which is also known as compliance function, is a description of the time variation of strain for a constant stress, and related to the molecular structure of the material, temperature and stress-time history (Covas et al. 2004). In Brunone et al. (2000) it is shown that very large (not physically reasonable) decay

66 coefficients of the friction formula (Brunone et al. 1995) should be used to simulate
67 transients in viscoelastic pipes when viscoelasticity is not taken into account.

68 In the frequency domain, most previous studies of fluid transient simulation in viscoelastic
69 pipelines used a frequency-dependent wave speed to describe the pipeline viscoelasticity,
70 and the modulus of elasticity of a viscoelastic pipeline was represented by the inverse of
71 the creep function (both in the frequency domain) (Meißner and Frank 1977; Rieutord 1982;
72 Franke and Seyler 1983; Suo and Wylie 1990). A diffident approach was taken by Duan et
73 al. (2012), which derived the transfer matrix of a viscoelastic pipeline, with and without a
74 leak, using the time-domain modified continuity equation and a one-element K-V model.
75 However, the frequency-dependent effects on the size of the resonant responses were not
76 observed in their numerical simulations, i.e. the resonant responses of the intact viscoelastic
77 pipe that was considered showed an almost uniform amplitude.

78 Research on the transient behavior of viscoelastic pipelines has also been extended to
79 numerical stability analysis of the MOC-based simulation with K-V model (Zecchin et al.
80 2008), viscoelastic pipelines with unsteady friction (Covas et al. 2005; Duan et al. 2010a;
81 Duan et al. 2010b), cavitation (Keramat et al. 2010), time-dependent Poisson's ratio
82 (Keramat et al. 2013), fluid structure interaction (Keramat et al. 2012), the presence of
83 leaks (Duan et al. 2012; Ferrante et al. 2013; Lazhar et al. 2013) and blockages (Meniconi
84 et al. 2012; Meniconi et al. 2013; Meniconi et al. 2014), and in networks (Zecchin et al.
85 2012).

With the interest of research on viscoelastic pipelines (in particular, pressurized polymeric water pipelines) gradually increasing in more complex scenarios and experimental studies, a critical issue is the accurate evaluation of the creep function, which is the key for accurate prediction of the mechanical behavior and transient response in real viscoelastic pipelines. The creep function of a viscoelastic pipeline can be evaluated by mechanical testing (Zhang and Moore 1997; Covas et al. 2004). However, experiments by Covas et al. (2004) showed that mechanical testing of small samples of the pipe wall material only provided an estimate of the actual mechanical behavior of the pipe system, which depends on not only the molecular structure of the material and temperature but also the pipe axial and circumferential constraints and stress-time history of the pipe system. An alternative approach is to calibrate the mechanical behavior of a pipeline system by hydraulic transient tests. Pezzinga and Scandura (1995) used a one-element K-V model to study a short additional HDPE pipeline connected to a relatively long steel pipeline system. The elastic modulus of elasticity (which corresponds to the elastic component of the pipe's circumferential expansion and manifested by the elastic wave speed) of the HDPE pipe was determined from the oscillation periods of the transient pressure wave, while the viscoelastic parameters were determined by trial-and-error. However, the accuracy of the calibration of the elastic modulus of elasticity (or the elastic wave speed) is hard to assure because the oscillation period is not constant over time in viscoelastic pipes due to wave dispersion. Covas et al. (2004) used the inverse transient analysis (ITA) (Liggett and Chen 1994) to calibrate the viscoelastic parameters of a HDPE pipeline by optimizing the parameters in a multi-element K-V model in order to minimizing the difference between the simulated and observed pressure traces. Unsteady friction was considered in the

109 forward modeling to account for the friction-induced damping. However, the elastic wave
110 speed (or the elastic creep) was not calibrated by ITA due to the non-uniqueness of the
111 solutions. It was estimated using the traveling time of the incident wave between two
112 pressure transducers, but the measured wave speed varied with the location of the
113 transducer pairs due to wave dispersion. The ITA approach was adapted in several later
114 studies (Soares et al. 2008; Duan et al. 2010a; Meniconi et al. 2012; Pezzinga 2014).
115 Keramat and Haghighi (2014) developed a 'viscoelastic Joukowsky formula' to describe
116 the head response in viscoelastic pipelines induced by a valve closure. Unsteady friction
117 was neglected in the formula. A curve-fitting procedure, which is much more
118 computational efficient than the ITA, was used to calibrate the mechanical parameters by
119 matching the numerical head response with the measurements in the first half water
120 hammer cycle. However, the elastic modulus of elasticity (or the elastic wave speed) was
121 not calibrated but pre-assigned in the case studies reported in Keramat and Haghighi (2014),
122 and the calibrated viscoelastic compliances were significantly different (20% or more)
123 from the values used in the original numerical model. Overall, all the previous hydraulic
124 transient-based studies on the calibration of the creep function of viscoelastic water
125 pipelines were limited to time-domain analysis. The parameter calibration, even for the
126 elastic modulus of elasticity (or the elastic wave speed) alone, is very challenging due to
127 the significant wave dispersion and the fact that unsteady friction also introduces wave
128 attenuation and dispersion.

129 The current research proposes a new technique for calibrating the creep function of
130 viscoelastic pipelines using hydraulic transients but with frequency-domain analysis. The
131 proposed technique only uses information about the resonant frequencies, which is not

subject to discrete faults (such as leaks) in pipelines. The analysis of the transfer matrix of a viscoelastic pipeline derived using a generalized multi-element K-V model shows that the use of an additional retarded strain term in the continuity equation and the use of a frequency-dependent wave speed (or frequency-dependent modulus of elasticity) to model the pipeline viscoelastic behavior are equivalent. It is also found that both the viscoelasticity and the unsteady friction introduce frequency-dependent reduction and shifting to the resonant response peaks of a pipeline system. Based on the analytical relationship between the resonant frequencies and the pipeline viscoelastic and friction-related parameters, a technique is developed to determine the elastic wave speed and the viscoelastic compliances from the resonant frequencies. The technique is complemented by an approach to correct the shifting in the resonant frequencies induced by the unsteady friction before the calibration of the viscoelastic parameters. Numerical case studies are conducted on an HDPE pipeline without and with unsteady friction. The results show that the new technique is computationally efficient and can yield accurate evaluation of the elastic wave speed and satisfactory accuracy for the viscoelastic compliances. Challenges for future applications in field pipelines are also identified and discussed in the end of the paper.

## Time-domain Governing Equations for Viscoelastic Pipelines

This section is a brief review of the time-domain governing equations for viscoelastic pipelines. The one-dimensional (1-D) momentum equation for transient flow in pressurized pipelines is given as (Wylie and Streeter 1993; Chaudhry 2014)

$$\frac{1}{gA}\frac{\partial Q}{\partial t}+\frac{\partial H}{\partial x}+h_f=0 \quad (1)$$

where $g$ is gravitational acceleration, $A$ is the cross-sectional area of a pipeline, $Q$ is the flow rate, $H$ is the piezometric head, $t$ is time, $x$ is distance along the pipeline, and $h_f$ is the head loss per unit length due to friction. The head loss can be regarded as a summation of a steady-state component and an unsteady-state component (Zielke 1968). The steady-state component is well defined for both laminar and turbulent flow (Wylie and Streeter 1993; Chaudhry 2014). Several unsteady head loss formulas are reported in the literature (Zielke 1968; Vardy et al. 1993; Brunone et al. 1995; Vítkovský 2006).

The one-dimensional continuity equation with a retarded strain term for viscoelastic pipelines is given as (Gally et al. 1979; Pezzinga and Scandura 1995; Covas et al. 2005)

$$\frac{gA}{a_e^{\,2}}\frac{\partial H}{\partial t}+\frac{\partial Q}{\partial x}+2A\frac{\partial \varepsilon_r}{\partial t}=0 \quad (2)$$

where $a_e$ is the elastic wave speed and $\varepsilon_r$ is the retarded strain. $a_e$ is related to the elastic modulus of elasticity $E_0$ by the classic wave speed formula (Wylie and Streeter 1993; Chaudhry 2014).

The generalized Kevin-Voigt (K-V) model has been commonly used to describe the mechanical behavior (creep function) of a viscoelastic material (Shaw and MacKnight 2005). The model, as illustrated in Figure 1, includes one elastic element and $N$

viscoelastic elements in series connection. The elastic element is represented by a single spring with a modulus of elasticity $E_0$ (which is referred as the elastic modulus of elasticity), and a viscoelastic element consists of a dashpot with a viscosity $\eta_k$ and a spring with a modulus of elasticity $E_k$ in parallel connection.

Using the K-V model, the creep function is described by

$$J(t) = J_0 + \sum_{k=1}^{N} J_k (1 - e^{-t/\tau_k}) \tag{3}$$

where $J_0$ equals $1/E_0$ and it is termed as the elastic creep in some literature, $J_k$ equals $1/E_k$ and it is the compliance of the spring of the $k$ th K-V element, $\tau_k$ equals $\eta_k / E_k$ and it is the retardation time of the dashpot of the $k$ th K-V element. Note that the K-V model is a phenomenological model without physical interpretation (Weinerowska-Bords 2006, 2007), as a result, different combinations of the number of K-V elements and the values of $J_0$, $J_k$ and $\tau_k$ may yield very similar creep curves (Covas et al. 2005; Keramat and Haghighi 2014). To reduce the possibility of non-uniqueness in solutions, a recent practice in research is to assume the number of K-V elements and assign constant values to $\tau_k$, then determine the values of $J_0$ and $J_k$ (Covas et al. 2005; Keramat and Haghighi 2014; Pezzinga 2014). This strategy is also used in the current research.

# Frequency-domain Governing Equations for Viscoelastic Pipelines

## *Transfer matrix for a viscoelastic pipeline*

The transfer function of a viscoelastic pipeline can be derived using the concept of steady-oscillatory flow, where every transient signal is described as a perturbation about a mean state (Wylie and Streeter 1993; Chaudhry 2014). Using Eqs. (1) and (2) and following the derivation presented in Duan et al. (2012) but using a generalized multiple element K-V model [Eq. (3)], the transfer matrix for a viscoelastic pipeline can be written as

$$\begin{Bmatrix} q \\ h \end{Bmatrix}^{n+1} = \begin{bmatrix} \cosh(\mu L) & -\frac{1}{Z}\sinh(\mu L) \\ -Z\sinh(\mu L) & \cosh(\mu L) \end{bmatrix} \begin{Bmatrix} q \\ h \end{Bmatrix}^{n} \tag{4}$$

where $q$ and $h$ are the complex flow and head oscillation in the frequency domain, $L$ is the total length of the pipe, and the propagation operator $\mu$ and the characteristic impedance $Z$ are given by

$$\mu = \frac{i\omega}{a_e} T_{VE} T_F \tag{5}$$

$$Z = \frac{a_e}{gA} \frac{T_F}{T_{VE}} \tag{6}$$

in which $\omega$ is the angular frequency, $T_{VE}$ and $T_F$ represent the terms contributed by viscoelasticity and friction, respectively, and are given as

$$T_{VE} = \sqrt{1 + a_e^2 \frac{\alpha D \rho}{e} \sum_{k=1}^{N} \frac{J_k}{i\omega\tau_k + 1}} \tag{7}$$

$$T_F = \sqrt{1 + \frac{gA}{i\omega} R} \tag{8}$$

where $\alpha$ is the pipeline restraint factor, $D$ is the pipeline internal diameter, $\rho$ is the density of fluid, $e$ is pipe wall thickness, $R$ is the resistance per unit length. More details for the derivation of Eqs. (5) to (8) can be found in Gong et al. (2015b).

$R$ can be described by a summation of the steady friction part $R_s$ and the unsteady friction part $R_{us}$, i.e. $R = R_s + R_{us}$, where $R_s = fQ_0 / (gDA^2)$ is the linearized steady-state resistance term for smooth-pipe turbulent flow and $f$ is the Darcy-Weisbach friction factor. The expression of $R_{us}$ presented in Vítkovský et al. (2003) is used in this research. The $R_{us}$ term was derived based on the Zielke (1968) unsteady friction model and the Vardy and Brown (1995; 1996) weighting function for smooth-pipe turbulent flow.

## *Modelling pipe viscoelasticity by retarded strain versus by complex wave speed*

A further analysis of Eqs. (5) and (6) shows that, the existing two approaches of modeling pipe wall viscoelastic effects on transient pressure waves as reported in literature [i.e. the

use of an additional term ( $2A\partial\varepsilon_r/\partial t$ ) to represent the retarded strain (Gally et al. 1979; Rieutord and Blanchard 1979; Güney 1983; Pezzinga and Scandura 1995; Ramos et al. 2004; Covas et al. 2005; Soares et al. 2008; Meniconi et al. 2012; Meniconi et al. 2014) and the use of a frequency-dependent and complex wave speed (Rieutord 1982; Suo and Wylie 1990)], are equivalent, despite apparent differences in their representations. In Rieutord (1982) and Suo and Wylie (1990), the pipeline viscoelasticity was modeled by only considering a frequency-dependent and complex modulus of elasticity $E(i\omega)$, which is defined as $1/J(i\omega)$ and $J(i\omega)$ is the frequency domain representation of the creep function shown in Eq.(3). The use of $E(i\omega)$ resulted in a frequency-dependent and complex wave speed $a^*$ as given by the classic wave speed formula for elastic pipes (Rieutord 1982; Suo and Wylie 1990)

$$a^* = \sqrt{\frac{K/\rho}{1+\alpha\left(K/E(i\omega)\right)\left(D/e\right)}} \tag{9}$$

To model the pipe wall viscoelastic effects for transient pressure waves, instead of the use of an additional term for the retarded strain, $a^*$ was used in the classic continuity equation for elastic pipes to replace the elastic wave speed (Rieutord 1982; Suo and Wylie 1990).

Considering the governing equations [Eqs. (5) and (6)] resulted from the use of an additional term for the retarded strain in the continuity equation, the ratio of $a_e$ to $T_{AE}$ can be regarded as a single parameter $a_c$. The use of $a_c$ also transforms the format of the

propagation operator $\mu$ [Eq. (5)] and the characteristic impedance $Z$ [Eq. (6)] to their counterparts for elastic pipes. $a_c$ in its full expression is written as

$$a_c = \frac{a_e}{\sqrt{1 + a_e^2 \frac{\alpha D \rho}{e} \sum_{k=1}^{N} \frac{J_k}{i\omega\tau_k + 1}}} \tag{10}$$

where the elastic wave speed $a_e$ is given by the classical wave speed formula for elastic pipes [same format as Eq. (9) but with a constant modulus of elasticity $E_0$]. Further mathematical arrangements show that $a_c$ as given in Eq. (10) is indeed the same as the frequency-dependent and complex wave speed $a^*$ as derived from the complex modulus of elasticity in Eq. (9). This finding indicates that the use of an additional viscoelastic term to represent the retarded strain is equivalent to the use of a frequency-dependent and complex wave speed (or modulus of elasticity) in the continuity equation. In other words, the mechanical characteristics of viscoelastic pipelines (an instantaneous elastic strain followed by a retarded strain) lead to a frequency-dependent wave speed. As a result, the pipeline viscoelasticity is more suitable to be analyzed in the frequency domain, where the pipe response to loadings with various frequencies can be studied independently.

## *Frequency response function of a viscoelastic pipeline*

The frequency response function (FRF) of a viscoelastic pipeline can be derived using the pipeline transfer matrix in Eq. (4) with boundary conditions. In this research, a reservoir-pipeline-high loss valve system is considered for the analytical derivation, and the special

case of a reservoir-pipeline-closed valve configuration is also studied in the numerical analysis. A side-discharge valve located just upstream of the high loss inline valve acts as the transient generator. Either discrete signals, such as a pulse (Lee et al. 2006), or continuous signals, such as pseudo random binary signals (Gong et al. 2015a), can be used as the excitation. In this research, a discrete discharge perturbation is considered as the input signal to the system, which can be realized by a fast successive opening and closing valve maneuver. The discharge perturbation then introduces head perturbations in the pipeline system, which are considered as the output of the system. Note that under linear system theory, for a system with a specific configuration, the system response function is independent of the format of the input excitation (or the type of valve maneuver provided the input is independent of the output). A discharge perturbation can be described by (Lee et al. 2006)

$$\begin{Bmatrix} q \\ h \end{Bmatrix}^{n+1} = \begin{bmatrix} 1 & 0 \\ 0 & 1 \end{bmatrix} \begin{Bmatrix} q \\ h \end{Bmatrix}^{n} + \begin{bmatrix} \Delta q \\ 0 \end{bmatrix} \tag{11}$$

where $\Delta q$ is the discharge perturbation induced by the valve.

Applying the transfer matrix method (Wylie and Streeter 1993; Chaudhry 2014) and the procedure used in elastic pipelines (Lee et al. 2006; Duan et al. 2012; Gong et al. 2013), the normalized complex head oscillation (frequency response function) at the downstream end of the pipeline (upstream side of the high loss valve) can be derived as

$$h^* = \frac{Z \tanh(\mu L)}{1 + \left[ Z \tanh(\mu L) / Z_V \right]} \tag{12}$$

where $h^*$ is the complex head oscillation normalized by the active input $\Delta q$, $Z_V$ is the impedance of the high loss inline valve, and $L$ is the length of the pipeline. Note that Eq. (12) is an expression of the normalized head response for either elastic or viscoelastic pipeline in a reservoir-pipeline-high loss valve system, and it is independent from the properties of the excitation. When the $T_{VE}$ and $T_F$ terms as defined in Eqs. (7) and (8) are used in $\mu$ and $Z$, the head response is for a viscoelastic pipeline with unsteady friction. The plot of the absolute value of Eq. (12) versus frequency is known as the Frequency Response Diagram (FRD) for the pipeline system, and the peaks (i.e. maxima) in the FRD are resonant responses of the system corresponding to the resonant frequencies (i.e. peak frequencies).

## Determination of the Creep Function using Resonant Frequencies

This section describes the proposed technique for calibrating the viscoelastic parameters in the creep function for viscoelastic pipelines. The technique is developed based on the analytical relationship between the resonant frequencies of a viscoelastic pipeline and the pipeline viscoelastic and friction-related parameters. As unsteady friction also contributes to the shifting of the resonant frequencies, an approach is developed to correct the effects induced by the unsteady friction before the calibration of the viscoelastic parameters.

## *Approach*

For an intact viscoelastic pipeline in a reservoir-pipeline-high loss valve system, the resonant responses are obtained when the absolute value of Eq. (12) reaches its maxima, where the corresponding frequencies are the resonant frequencies. When the inline valve is a high loss valve or fully closed so that the value of $Z_V$ is much greater than the value of $\left|Z\tanh(\mu L)\right|$, Eq. (12) can be simplified as

$$h^* = Z\tanh(\mu L) \tag{13}$$

with negligible impacts on the resonant frequencies.

The characteristic impedance $Z$ is a frequency-dependent function and related to the viscoelastic and friction terms, but its values are unknown when the viscoelastic parameters are unknown. Numerical simulations show that $Z$ is a monotonic function of frequency (presented later in Figure 7). To simplify the analysis, an assumption is made that the influence of $Z$ on the maxima or minima of Eq. (13) can be neglected (implications are further discussed in the later section *Discussions*). In other words, it is assumed that the measured resonant frequencies [which are actually the peak frequencies of the function in Eq. (12)] are the frequencies where the function $\left|\tanh(\mu L)\right|$ reaches its maxima.

From the mathematic properties of hyperbolic functions (Kreyszig et al. 2011), the hyperbolic tangent is periodic with respect to the imaginary component and the period is $\pi i$, where $i$ represents the imaginary unit. For a complex hyperbolic tangent function

297 $\tanh(x+yi)$ with a specific real part $x$, the maxima of the absolute value of the function
298 (i.e. $|\tanh(x+yi)|$) are obtained when the imaginary part $y$ is an odd multiple of $\pi/2$. A
299 3D mesh plot of function $|\tanh(x+yi)|$ is given in Figure 2.

300 The real and the imaginary parts of the propagation operator $\mu$ are monotonic functions
301 of frequency. The results of $|\tanh(\mu L)|$ for the practical HDPE pipeline considered in the
302 *Case Studies* section are shown as the thick line in Figure 2, which can be considered as a
303 curved slice of the 3D mesh. It can be seen that the maxima of the function $|\tanh(\mu L)|$ are
304 achieved at specific frequencies where the imaginary part of the variable are odd multiples
305 of $\pi/2$, i.e.

$$\mathrm{Im}\left[\mu(\omega_m)L\right] = (2m-1)\frac{\pi}{2} \tag{14}$$

306 where Im[ ] signifies the imaginary part of the complex number in the brackets, $\omega_m$
307 represent the resonant angular frequencies, $m$ is an integer ($m$ = 1, 2 , 3 …) and represents
308 the ordinal number of the resonant peaks.

309 Substituting Eq. (5) into Eq. (14) and applying mathematical manipulation yields

$$\omega_m = (2m-1)\frac{a_e \pi}{\mathrm{Re}\left[T_{VE}(\omega_m)T_F(\omega_m)\right]2L} \tag{15}$$

where $\mathrm{Re}[\ ]$ signifies the real part of the complex number in the brackets. Eq. (15) shows that the resonant frequencies of a viscoelastic pipeline is a function of the elastic wave speed $a_e$, the viscoelastic term $T_{VE}$, the friction term $T_F$ and the length of pipe $L$. As a result, it is possible to calibrate the value of $a_e$ (which is related to the elastic creep $J_0$) and the viscoelastic parameters in $T_{VE}$ and the friction-related parameters in $T_F$ by using known resonant (angular) frequencies $\omega_m$, which can be read from a measured FRD as the peak frequencies. By this approach, the calibration of the viscoelastic parameters in $T_{VE}$ is transferred to a problem of solving a set of nonlinear equations, defined by Eq. (15), and the number of equations to be used depends on the number of unknown parameters to calibrate.

## *Steps for implementation*

The effects of viscoelasticity and friction on the resonant frequencies are coupled as the product of $T_{VE}$ and $T_F$, which means the solutions may be non-unique if both $T_{VE}$ and $T_F$ are open to calibration. Previous research on elastic pipelines (Lee et al. 2006; Sattar and Chaudhry 2008) concluded that steady friction does not change the resonant frequencies, while the influence of unsteady friction on the resonant frequencies is very limited. Numerical simulations conducted in this research (as shown later in the *Case Studies* section) confirm those findings. However, the current research also discovers that, although neglecting the effects of unsteady friction in a viscoelastic pipeline does not impose much impact on the calibration of the elastic wave speed, it can have a significant impact on the calibration of the viscoelastic compliances, especially for the high order K-V elements. The

331 explanation is that the higher the order an element is in the K-V model, the less influence
332 it has to the hydraulic behavior of the pipeline system. This means the elastic modulus of
333 elasticity, or the elastic wave speed, is the dominant factor and has the greatest influence
334 on the resonant frequencies, while the influence of the viscoelastic compliances decreases
335 with the increase in element order. It is also evident from the definition of the creep function
336 in Eq. (3), where the relative variation in $J(t)$ is less sensitive to the relative variation in
337 the value of higher order $J_k$. From the perspective of parameter calibration using measured
338 resonant frequencies, the calibration of the elastic compliance is the least sensitive to errors
339 in the measured resonant frequencies, while the sensitivity to error increases with the
340 increase in the order of K-V elements. In other words, it is more difficult to accurately
341 calibrate higher order K-V elements, because a relatively small error in the measured
342 resonant frequencies would have to be explained by a relatively greater change in the higher
343 order $J_k$ values.

344 This research proposes a multi-step strategy to implement the calibration of the elastic
345 wave speed and the viscoelastic compliances. The FRD of a viscoelastic pipeline in a
346 reservoir-pipeline-high loss valve system can be extracted by hydraulic transient tests and
347 the resonant frequencies are determined by locating the peaks in the FRD. Without loss of
348 generality, a high loss inline valve is considered, although a fully closed inline valve is
349 preferred. The resonant frequencies are shifted due to unsteady friction and viscoelasticity
350 when compared with those in a theoretical frictionless and elastic pipe. As the calibration
351 of the viscoelastic parameters is the focus, an approach is proposed to correct the shifting
352 of the resonant frequencies induced by the effects of unsteady friction before the ultimate

calibration for the viscoelastic parameters. The elastic wave speed and the viscoelastic compliances are firstly estimated from the originally measured resonant frequencies by solving Eq. (15) with neglecting the effects of friction (i.e. $T_F = 1$). Considering that the shifting in resonant frequencies due to the unsteady friction is insignificant, the estimated wave speed should be close to the true elastic wave speed, though the estimated viscoelastic compliances may have significant error. Using this estimated elastic wave speed and the friction factor estimated from the steady state, numerical simulations can be conducted to estimate the resonant frequencies for the scenario elastic and frictionless (EL) and the scenario elastic with unsteady friction (EL+UF). The contribution of the unsteady friction to the shifting of the resonant frequencies can be evaluated from the numerical results, and then corrected from the measured resonant frequencies. The corrected resonant frequencies, with the unsteady friction-induced shifting largely corrected, are then used in Eq. (15) for the calibration of the elastic wave speed and the viscoelastic compliances. The detailed procedure for the systematic evaluation of the elastic wave speed and the viscoelastic compliances is summarized in the following steps:

1. For a viscoelastic pipeline in a reservoir-pipeline-high loss valve configuration, determine the Darcy-Weisbach friction factor $f$ using the steady-state head loss, and the Reynolds number $\mathtt{R}$ from the steady-state flow.
2. Extract the frequency response diagram (FRD) of the viscoelastic pipeline system. Techniques for FRD extraction in real pipelines can be found in Lee et al. (2006; 2008) and Gong et al. (2015a). The resonant frequencies, $\omega_m$, are then read from the measured FRD by locating the peaks of the pressure response.

3. Solve the set of nonlinear equations defined by Eq. (15) for $m = 1, \cdots, M$, neglecting the influence of the friction term (i.e. $T_F$ = 1) to estimate the elastic wave speed $a_e$ and the viscoelastic compliances $J_k$. The number of equations $M$ (the number of resonant frequencies used in the parameter calibration) has to be equal or more than the number of unknown parameters. For example, if a three-element K-V model is used and $\tau_k$ are fixed to reduce the possibility of non-uniqueness in solutions, as adopted in other studies (Covas et al. 2005; Soares et al. 2008; Keramat and Haghighi 2014), there are four unknowns to determine, including $a_e$, $J_1$, $J_2$ and $J_3$. As a result, four or more resonant frequencies in the measured FRD should be used. The values of $\tau_k$ used should be significantly different from one another and all smaller than one half the fundamental pipeline period (see the sub-section *Retardation time and pipe period* later in this paper for more discussion).
4. Calculate the resonant frequencies using Eq. (15) neglecting both the effects of viscoelasticity and friction (i.e. $T_{VE}$ = 1 and $T_F$ = 1) for a corresponding frictionless and elastic pipeline system. This is achieved by substituting the elastic wave speed $a_e$ determined in Step 3 into Eq. (15). The results, symbolized as $\omega_{m\_FL}$, are the estimated resonant frequencies for the corresponding frictionless and elastic pipeline system.
5. Calculate the resonant frequencies using Eq. (15) neglecting the effects of viscoelasticity (i.e. $T_{VE}$ = 1) for a corresponding elastic pipeline system with unsteady friction. This is achieved by substituting the Darcy-Weisbach friction

factor $f$ and the Reynolds number $\mathbf{R}$ determined in Step 1 and the elastic wave speed $a_e$ determined in Step 3 into Eq. (15). The results, symbolized as $\omega_{m\_UF}$, are the estimated resonant frequencies for the corresponding elastic pipeline with unsteady friction.

6. Correct the measured resonant frequencies obtained in Step 2 to remove the shifting induced by unsteady friction. The correction is achieved by the formula

$$\omega_{m\_C} = \omega_m \frac{\omega_{m\_FL}}{\omega_{m\_UF}} \tag{16}$$

where $\omega_{m\_C}$ represents the corrected resonant frequencies. $\omega_{m\_C}$ is a good approximation of the resonant frequencies for the corresponding frictionless viscoelastic pipeline.

7. Repeat Step 3 to determine $a_e$ and $J_k$ but use the corrected resonant frequencies $\omega_{m\_C}$ obtained in Step 6.

The effectiveness of the proposed procedure is verified by numerical simulations, as presented in the section of *Case Studies*.

## Case Studies

Numerical simulations are conducted for an HDPE pipeline bounded by a reservoir and an inline valve to verify the proposed technique for the calibration of the creep function (the elastic wave speed and the viscoelastic compliances). A discharge perturbation [defined in

Eq. (11)] is used as the transient excitation, which can be realized by abruptly opening and then closing a side-discharge valve located just upstream of the inline valve. Two case studies are considered: one is a reservoir-pipeline-closed valve system without friction and another is a reservoir-pipeline-high loss valve system with the consideration of unsteady friction.

## *System specifications*

The physical details of the pipeline system, as given in Table 1, are adapted from the experimental pipeline in the Imperial College as reported in Covas et al. (2004), but the length of the pipe is doubled in the Case Studies to ensure all creep elements fully act within half period of a water hammer cycle so that they are possible to be calibrated (more discussion in the later sub-section *Retardation time and pipe period*). Note that the steady-state flow rate 0.3 L/s is for the reservoir-pipeline-high loss valve configuration (case study 2) and it is zero for the configuration where the inline valve is fully closed (case study 1). The elastic wave speed $a_e$, which is to be calibrated, is 395 m/s and given in Table 1. The viscoelastic parameters are from one of the experimentally calibrated results in Covas et al. (2004), and they are given in Table 2. Research by Covas et al. (2004) showed that the use of three viscoelastic elements in the K-V model is sufficient enough to describe the viscoelasticity of a HDPE pipeline. The compliance coefficients $J_1$ to $J_3$ are to be determined by the proposed technique.

## *Case study 1: reservoir-pipeline-closed valve*

The reservoir-pipeline-closed valve configuration is the suggested configuration for the calibration of the pipeline viscoelastic parameters. The effects of friction are small because of the zero steady-state flow and Eq. (13), in which the impedance of the valve is not involved, is the governing equation for the frequency response function of the system. A frictionless pipeline is considered in this case study.

### Theoretical frequency response diagrams

Using Eq. (13) and neglecting friction, the theoretical frequency response diagrams (FRDs) for the scenarios: (a) elastic and frictionless (EL) and (b) viscoelastic and frictionless (VE) are obtained and illustrated in Figure 3. For the scenario of EL (solid line in Figure 3), the resonant responses are infinite and therefore cannot be fully shown in the figure. The first four resonant angular frequencies for the two FRDs respectively are read and given in Table 3. It can be seen from Figure 3 and Table 3 that the pipe wall viscoelasticity introduces non-uniform shifting of the resonant frequencies and non-uniform reduction of the amplitude of the resonant responses.

### Parameter evaluation

The calibration of the elastic wave speed $a_e$ and the viscoelastic parameters $J_1$ to $J_3$ is relatively easy when the effect of friction is negligible. The procedure is as described in Steps 1 to 3 in the sub-section *Steps for implementation.* Once the first four resonant frequencies $\omega_m$ ($m$ = 1 to 4) are determined (as given in Table 3), four nonlinear equations can be established from Eq. (15). Solving the four nonlinear equations gives the elastic

455 wave speed $a_e$ and the viscoelastic parameters $J_1$ to $J_3$ and the results are summarized in
456 Table 4. In this research, the shuffled complex evolution (SCE) algorithm (Duan et al. 1993)
457 is used to search the values for $a_e$ and $J_1$ to $J_3$ by minimizing the objective function

$$F(a_e, J_k) = \sum_{m=1}^{M} \left[ \frac{\omega_m |T_{VE}|}{a_e (2m-1)} - \frac{\pi}{2} \right]^2 \quad (16)$$

458 Note that $T_{VE}$ is given in Eq. (7) and is a function of $a_e$ , $J_k$ and $\omega_m$ . The search space is
459 limited to the range of [350, 450] for $a_e$ and [1E−11, 1E−9] for the $J_k$ , as these are
460 physically plausible ranges for a HDPE pipe according to the study by Covas et al. (2005).

461 It can be seen from Table 4 that the calibrated results are very close to the theoretical results
462 used in the original model. The difference is due to the simplifications and approximations
463 used in the derivation of Eq. (15). The calibrated FRD is compared with the theoretical
464 FRD for the scenario of viscoelastic and frictionless in Figure 4. The close similarity
465 between the calibrated and the theoretical FRDs indicates that the calibrated results can
466 appropriately represent the viscoelastic behavior of the pipeline system. Case study 1
467 verifies that the proposed technique is valid for a frictionless viscoelastic pipeline.

## 468 *Case study 2: reservoir-pipeline-high loss valve*

469 The reservoir-pipeline-high loss valve configuration is studied in this case study. Due to
470 the existence of steady-state flow, the effects of friction are typically not negligible in the

calibration of the viscoelastic parameters. Eq. (12) is the governing equation for the frequency response function of the system.

## Theoretical frequency response diagrams

The theoretical frequency response diagrams (FRDs) of the reservoir-pipeline-high loss valve system are simulated by Eq. (12) for the scenarios: (a) elastic and frictionless (EL); (b) elastic with steady and unsteady friction (EL+UF); (c) viscoelastic and frictionless (VE); and (d) viscoelastic with steady and unsteady friction (VE +UF), and the results are given in Figure 5. The first four resonant angular frequencies for the four FRDs respectively are read and given in Table 5.

It can be seen from Figure 5 and Table 5 that both the unsteady friction and the viscoelasticity shift the resonant frequencies of the pipeline system, although the shifting induced by the unsteady friction is much less than that induced by the viscoelasticity. The scenario of VE +UF experiences the greatest shifting from the theoretical resonant frequencies of the EL case. The numerical results also confirm that both the unsteady friction and the viscoelasticity can introduce non-uniform reduction in the size of the resonant responses.

## Parameter evaluation

The elastic wave speed $a_e$ and the viscoelastic compliances $J_1$ to $J_3$ are determined using the procedure proposed in the sub-section *Steps for implementation*. In addition to the steady-state hydraulic condition, it is assumed that only the FRD (or the resonant

491 frequencies) of the scenario of VE+UF is known because this is the scenario for a real
492 reservoir-pipeline-high loss valve system.

493 Estimate the elastic wave speed neglecting friction:

494 The elastic wave speed is estimated using the measured resonant frequencies by following
495 the instructions in Steps 1 to 3. Four equations are established using Eq. (15) for $m$ = 1 to
496 4. The SEC is used to solve the equations and the results of the calibration using the
497 resonant frequencies from the scenario VE+UF and neglecting the effect of friction are
498 given in Table 6. The result for the elastic wave speed $a_e$ is very close to the value of 395
499 m/s used in the original model. The calibrated $J_k$ have significant discrepancies from the
500 values used in the original model, which indicates that the effects of friction cannot simply
501 be neglected in the calibration process for this case study.

502 Correct the shifting in resonant frequencies induced by unsteady friction:

503 Steps 4 to 6 are conducted to correct the effects of unsteady friction on the shifting of the
504 resonant frequencies. The approximation of the resonant angular frequencies ($\omega_{m\_C}$) for
505 the viscoelastic and frictionless (VE) scenario is obtained, and the results are given in Table
506 7. The resonant angular frequencies for the scenarios of EL and EL+UF are calculated
507 using Eq. (15) with the elastic wave speed $a_e$ = 396.9 m/s as calibrated in Step 3. The
508 approximation of the resonant angular frequencies ($\omega_{m\_C}$) for scenario VE is obtained from
509 Eq. (16). It can be seen that the estimated resonant frequencies is very close to the

theoretical results for the scenario VE shown in Table 5 where unsteady friction is not included in the model.

Calibration using the corrected resonant frequencies:

The final stage for the parameter evaluation is the Step 7 in the proposed procedure. The estimated resonant frequencies for the scenario VE are substituted into Eq. (15) and the SCE algorithm is run to obtain the results, which are presented in Table 8. The results show that the elastic wave speed and the viscoelastic compliances are all calibrated with acceptable accuracy compared with the values used in the original pipeline model. The viscoelastic compliances are much better calibrated when compared with the results in Table 6, where the effects of friction were simply neglected. The significant improvement in accuracy verifies that the proposed approach for correcting the effects of unsteady friction is useful.

The FRD for the scenario viscoelastic and frictionless (VE) is simulated using Eq. (12) with the calibrated parameters in Table 8. The results are given in Figure 6 as the dashed line, with the comparison to the theoretical FRD for scenario VE (the solid line) obtained from the values of these parameters in the original model. A generally good match is observed in Figure 6 between the calibrated FRD and the theoretical FRD, which indicates that the calibrated parameters can be used to describe the viscoelastic characteristics of the pipeline system.

# Discussions

The outlined numerical case study shows that the proposed technique for the calibration of the creep function of viscoelastic pipelines is effective even when unsteady friction is present. However, a few practical issues that may bring challenges in future field applications are identified and discussed as follows:

## *Retardation time and pipe period*

The proposed technique calibrates the elastic wave speed and the viscoelastic compliances based on resonant frequencies and a set of preselected retardation times. The numerical *Case Studies* reported in a previous section used a pipe length two times that in the original laboratory pipeline system in Covas et al. (2004). The increase in length was adopted to ensure that the pipe is long enough that all the K-V elements have enough time (within the half period of any water hammer cycle) to significantly respond before a change in the pressure loading. Research in the time domain showed that compliances with a retardation time greater than one half the period are unable to be calibrated with accuracy because the retardation effects from them are not fully expressed before a change in loading (Keramat and Haghighi 2014). In the *Case Studies*, the viscoelastic parameters are kept the same as those in Covas et al. (2004) so that the viscoelastic properties of the pipeline are kept the same. The third retardation time $\tau_3$ is 1.5 s and is greater than one half the period of the water hammer cycle (approximately 1.4 s as estimated by $2L/a_e$) if the original pipe length of 277 m is used. As a result, the pipe length was doubled in the *Case Studies* to make sure all the K-V elements can fully respond within one half the period of the water hammer cycle.

551 Extra numerical simulations are conducted in this research after modifying the length of
552 the pipe to 277 m [the original length of the laboratory system in Covas et al. (2004), half
553 the length considered in the *Case Studies* section]. A reservoir-pipeline-closed valve
554 configuration is considered and the pipeline is assumed as frictionless in the original model.
555 While keeping the viscoelastic compliances ($J_1$ to $J_3$) the same as those used in the *Case*
556 *Studies*, two sets of retardation time ($\tau_1$ to $\tau_3$) are used to generate two theoretical FRDs
557 by Eq. (13). The first set are the same as those used in the *Case Studies* and they are $\tau_1$ =
558 0.05 s, $\tau_2$ = 0.5 s and $\tau_3$ = 1.5 s. The second set are $\tau_1$ = 0.05 s, $\tau_2$ = 0.25 s and $\tau_3$ = 1.0
559 s so that the retardation time are significantly different from one another and all are smaller
560 than one half the period of the water hammer cycle (approximately 1.4 s). Two sets of the
561 elastic wave speed and the viscoelastic compliances are then calibrated from the two
562 theoretical FRDs by following the Steps 1 to 3 presented in the sub-section *Steps for*
563 *implementation* (same procedure as used in Case study 1). The results are summarized in
564 Table 9.

565 Comparing the results shown in Table 9 with the results of the previous Case study 1 in
566 Table 4, it can be seen that when the length of the pipe is changed from 554 m (Table 4) to
567 277 m (Table 9) but the viscoelastic parameters are all kept the same, $J_2$ and $J_3$ cannot be
568 calibrated with acceptable accuracy because the $\tau_3$ is greater than one half the period of
569 the water hammer cycle. However, when the second set of the retardation times ($\tau_1$ = 0.05
570 s, $\tau_2$ = 0.25 s and $\tau_3$ = 1.0 s) are used in the original model and also in the calibration
571 process, all the viscoelastic compliances are calibrated with high accuracy. Several other

sets of retardation times that satisfy the criteria "significantly different from one another and all smaller than one half the period of the water hammer cycle" are also studied and they all yield successful calibration.

The numerical simulations confirm that the selection of the set of retardation times is critical for the calibration of viscoelastic compliances. For a real viscoelastic pipeline with a specific length and elastic wave speed, the set of retardation times should be selected as significantly different from one another and all smaller than one half the period of the water hammer cycle. Further analysis on the importance of pipe system scale, in particular pipe length and diameter, on viscoelastic behavior in pipe transients is suggested for future research.

## *Influence of the characteristic impedance*

In the proposed parameter evaluation technique, it is assumed that the measured resonant frequencies (which are actually the peak frequencies of the function $\left|Z\tanh(\mu L)\right|$) are the frequencies where the function $\left|\tanh(\mu L)\right|$ reaches its maxima. This inevitably introduces error into the parameter calibration because $Z$ is a frequency-dependent function rather than a constant number. As defined in Eq. (6), the values of $Z$ depend on the viscoelastic and the friction terms, and they are typically unknown or have great uncertainties for real pipeline applications. As a result, the effects from $Z$ on the resonant frequencies are difficult to assess or correct before the parameter calibration.

591 However, the values of $Z$ are calculated numerically for the pipeline system discussed in
592 the *Case Studies*, and its absolute values are plotted in Figure 7. The effects of $Z$ is
593 evaluated for the *Case Studies* by calculating the difference between the peak frequencies
594 of $\left|Z\tanh(\mu L)\right|$ and those of $\left|\tanh(\mu L)\right|$, both for the VE scenario, and the results are given
595 in Figure 8.

596 It can be seen from Figure 7 that $Z$ is a monotonic function of frequency. From Figure 8,
597 the differences in the peak frequencies between the functions $\left|Z\tanh(\mu L)\right|$ and $\left|\tanh(\mu L)\right|$
598 are observed to be small. Numerical simulations in Case study 1 showed that the effects of
599 the assumption on the determination of the elastic wave speed and the viscoelastic
600 compliances are small (the maximum relative error induced was less than 4% as shown in
601 Table 4). A more detailed analysis of the influence of $Z$ is recommended for future
602 research.

## 603 *Determination of the resonant frequencies*

604 The successfully application of the proposed technique relies on the accurate determination
605 of the resonant frequencies of a pipeline system. The determination of the resonant
606 frequencies typically requires the extraction of the frequency response diagram (FRD).
607 Two challenges exist (which also apply to all FRD-based techniques): the bandwidth of the
608 transient excitation and the specific boundary condition required (Lee et al. 2013).
609 Fortunately, the proposed technique for the calibration of the creep function only requires
610 the first few resonant peaks to be measured and viscoelastic pipelines typically has a low
611 fundamental frequency due to low wave speeds. Consider the pipeline used in the *Case*

612 *Studies* as an example (a 557 m HDPE pipe with an elastic wave speed of 395 m/s), the
613 bandwidth of the transient excitation is required to be just higher than 1.2 Hz, which is easy
614 to achieve even by a manual valve closure. The specific boundary condition required for
615 the proposed technique is a reservoir-pipeline-valve (RPV) configuration. This is typically
616 not readily available in complex pipeline networks. Lee et al. (2005) proposed a technique
617 to subdivide complex systems into individual single pipes for the purpose of FRD
618 extraction by using a close in-line valve and a junction as the boundaries. The side-
619 discharge valve-based transient generator recently developed by the authors (Gong et al.
620 2015a) can be useful in extracting the FRD of a viscoelastic pipeline by using persistent
621 pseudo random binary signals. However, experimental verification is needed in the future.

622 ## *Effects of complexities in real pipelines*

623 In addition to frictional effects, real pipelines may have complexities such as faults and
624 significant fluid structure interaction (FSI). Studies on elastic pipelines show that the
625 influence of discrete faults, including leaks and discrete blockage, on the resonant
626 frequencies of a pipeline system is negligible (Lee et al. 2005). However, extended wall
627 deterioration, such as extended blockages, can slightly alter the resonant frequencies (Lee
628 et al. 2013). FSI, in particular the axial oscillation of the pipeline during transient events,
629 may also have some impact on the resonant frequencies (Keramat et al. 2012), but the
630 details are yet to be explored in the future.

# Conclusions

A new technique has been proposed for calibrating the elastic wave speed and the viscoelastic compliances in viscoelastic pipelines using hydraulic transient analysis, which is the first viscoelastic parameter estimation technique developed in the frequency domain. The transfer matrix of a viscoelastic pipeline, with steady and unsteady friction considered, has been derived from the time-domain one-dimensional continuity and momentum water hammer equations, where an extra viscoelastic term is included in the continuity equation to represent the retarded strain. A generalized Kelvin-Voigt (K-V) model with multiple viscoelastic elements is used to describe the creep function. It has been found that the use of a viscoelastic term in the continuity equation in the time-domain is equivalent to the use of a frequency-dependent complex wave speed (or modulus of elasticity) in the frequency-domain. The frequency response function (FRF) of a viscoelastic pipeline in a reservoir-pipeline-high loss valve configuration has been derived, from which the relationship between the resonant frequencies and the pipeline elastic wave speed and viscoelastic compliances are analytically established. A parameter calibration technique has been proposed for the evaluation of these parameters using the resonant frequencies. Detailed steps for implementing the technique have been presented, including an approach for correcting the shifting in resonant frequencies induced by unsteady friction. The parameter evaluation is achieved by solving a set of nonlinear equations, which is much more computational efficient (less than 2 s in this study for solving four equations using the shuffled complex evolution algorithm) than the conventional inverse transient analysis (ITA)-based parameter calibration. For the first time, the elastic wave speed is calibrated together with the viscoelastic compliance in the frequency domain, rather than being

654 estimated separately in the time domain. The proposed technique only uses information
655 about the resonant frequencies, which is not subject to discrete faults (such as leaks) in
656 pipelines.

657 Numerical case studies have been conducted on an HDPE pipeline to verify the proposed
658 technique. A three K-V element model has been used to simulate the pipeline viscoelastic
659 effects. For a frictionless pipeline (case study 1), the elastic wave speed and viscoelastic
660 compliances are calibrated with high accuracy (less than 4 % relative error compared with
661 the theoretical values used in the original pipeline model). When unsteady friction is
662 considered (case study 2), the approach correcting the unsteady friction-induced shifting
663 of the resonant frequencies is proved to be useful and significantly improves the accuracy
664 of the calibration. It is also worth noting that the elastic wave speed can be calibrated with
665 a high accuracy (less than 1% relative error compared with the theoretical value) no matter
666 whether the effect of unsteady friction is corrected or not. Practical issues that may bring
667 challenges in future field applications, including the selection of the retardation times, the
668 influence of the characteristic impedance, the determination of the resonant frequencies
669 and some complexities in real pipeline systems, have been discussed in the section
670 *Discussions* in the paper.

671 Overall, the proposed frequency-domain technique is a step forward towards accurate
672 calibration of the creep function of viscoelastic pipelines. The elastic wave speed and the
673 viscoelastic compliances can be calibrated with satisfactory accuracy provided that a few
674 resonant frequencies of a viscoelastic pipeline system are known.

## Acknowledgements

The research presented in this paper has been supported by the Australia Research Council through the Discovery Project Grant DP140100994.


## Notation

*The following symbols are used in this paper:*

$A$ = pipe cross sectional area ($m^2$);

$a_c$ = frequency-dependent complex wave speed derived from the use of retarded strain term (−);

$a_e$ = elastic wave speed (m/s);

$a^*$ = frequency-dependent complex wave speed derived from complex modulus of elasticity (−);

$D$ = internal pipe diameter (m);

$E_0$ = elastic modulus of elasticity (Pa);

$E_k$ = modulus of elasticity for the $k$ th viscoelastic element (Pa);

$e$ = wall thickness of a pipe (m);

$F(\ )$ = objective function (−);

$f$ = Darcy-Weisbach friction factor (−);

$g$ = gravitational acceleration ($ms^{-2}$);

$H$ = piezometric head (m);

$H_0$ = steady-state head (m);

$h$ = complex head oscillation (m);

$h_f$ = head loss per unit length due to friction (m);

$h^*$ = normalized complex head oscillation ($m^{-2}s$);

$i$ = imaginary unit (−);

$J(\ )$ = creep (compliance) function ($Pa^{-1}$);

$J_0$ = elastic compliance, $E_0^{-1}$ ($Pa^{-1}$);

$J_k$ = viscoelastic compliance, $E_k^{-1}$ ($Pa^{-1}$);

$L$ = length of pipe (m);

$M$ = total number of resonant frequencies used (−);

$N$ = total number of viscoelastic elements used (−);

$Q$ = flow rate ($m^3s^{-1}$);

$q$ = complex flow oscillation ($m^3s^{-1}$);

$R$ = resistance coefficient ($sm^{-3}$);

$R_s$ = resistance from steady friction ($sm^{-3}$);

$R_{us}$ = resistance from unsteady friction ($sm^{-3}$);

$\mathbf{R}$ = Reynolds number (−);

$T_F$ = friction term in the characteristic impedance and propagation operator (−);

$T_{VE}$ = viscoelastic term in the characteristic impedance and propagation operator (−);

$t$ = time (s);

$x$ = spatial coordinate (m);

$Z$ = characteristic impedance ($m^{-2}s$);

680

681 *Greek symbols:*

$\Delta q$ = discharge perturbation ($m^3/s$);

$\alpha$ = pipeline restraint factor (−);

$\varepsilon_r$ = total retarded strain (−);

$\eta_k$ = viscosity for the $k$ th viscoelastic element;

$\mu$ = propagation operator ($m^{-1}$);

$\rho$ = fluid density ($kgm^{-3}$);

$\tau_k$ = retardation time for the $k$ th viscoelastic element (s);

$\omega$ = angular frequency (rad);

$\omega_m$ = resonant angular frequency (rad);

$\omega_{m\_C}$ = approximation of the resonant angular frequency for a frictionless viscoelastic pipeline (rad);

$\omega_{m\_EL}$ = calculated resonant angular frequency for a frictionless elastic pipeline (rad);

$\omega_{m\_UF}$ = calculated resonant angular frequency for an elastic pipeline with steady and unsteady friction (rad);

682

# 683 References


684 Brunone, B., Golia, U. M., and Greco, M. (1995). "Effects of two-dimensionality on pipe
685 transients modeling." *Journal of Hydraulic Engineering*, 121(12), 906-912.
686 Brunone, B., Karney, B. W., Mecarelli, M., and Ferrante, M. (2000). "Velocity profiles
687 and unsteady pipe friction in transient flow." *Journal of Water Resources*
688 *Planning and Management*, 126(4), 236-244.

689 Brunone, B., and Berni, A. (2010). "Wall Shear Stress in Transient Turbulent Pipe Flow
690 by Local Velocity Measurement." *Journal of Hydraulic Engineering*, 136(10),
691 716-726.
692 Chaudhry, M. H. (2014). *Applied Hydraulic Transients*, 3rd Ed., Springer, New York,
693 NY.
694 Covas, D., Stoianov, I., Mano, J. F., Ramos, H., Graham, N., and Maksimovic, C. (2004).
695 "The dynamic effect of pipe-wall viscoelasticity in hydraulic transients. Part I -
696 Experimental analysis and creep characterization." *Journal of Hydraulic*
697 *Research*, 42(5), 516-530.
698 Covas, D., Stoianov, I., Mano, J. F., Ramos, H., Graham, N., and Maksimovic, C. (2005).
699 "The dynamic effect of pipe-wall viscoelasticity in hydraulic transients. Part II -
700 Model development, calibration and verification." *Journal of Hydraulic Research*,
701 43(1), 56-70.
702 Duan, H.-F., Ghidaoui, M., Lee, P. J., and Tung, Y.-K. (2010a). "Unsteady friction and
703 visco-elasticity in pipe fluid transients." *Journal of Hydraulic Research*, 48(3),
704 354-362.
705 Duan, H.-F., Ghidaoui, M. S., and Tung, Y.-K. (2010b). "Energy analysis of
706 viscoelasticity effect in pipe fluid transients." *Journal of Applied Mechanics,*
707 *Transactions ASME*, 77(4), 1-5.
708 Duan, H.-F., Lee, P. J., Ghidaoui, M. S., and Tung, Y.-K. (2012). "System response
709 function-based leak detection in viscoelastic pipelines." *Journal of Hydraulic*
710 *Engineering*, 138(2), 143-153.
711 Duan, Q. Y., Gupta, V. K., and Sorooshian, S. (1993). "Shuffled complex evolution
712 approach for effective and efficient global minimization." *Journal of Optimization*
713 *Theory and Applications*, 76(3), 501-521.
714 Ferrante, M., Massari, C., Brunone, B., and Meniconi, S. (2013). "Leak behaviour in
715 pressurized PVC pipes." *Water Science and Technology: Water Supply*, 13(4),
716 987-992.
717 Franke, P. G., and Seyler, F. (1983). "Computation of unsteady pipe flow with respect to
718 visco-elastic material." *Journal of Hydraulic Research*, 21(5), 345-353.
719 Gally, M., Güney, M., and Rieutord, E. (1979). "An Investigation of Pressure Transients
720 in Viscoelastic Pipes." *Journal of Fluids Engineering*, 101(4), 495-499.
721 Gong, J., Lambert, M. F., Simpson, A. R., and Zecchin, A. C. (2013). "Single-event leak
722 detection in pipeline using first three resonant responses." *Journal of Hydraulic*
723 *Engineering*, 139(6), 645-655.
724 Gong, J., Lambert, M. F., Zecchin, A. C., and Simpson, A. R. (2015a). "Experimental
725 verification of pipeline frequency response extraction and leak detection using the
726 inverse repeat signal." *Journal of Hydraulic Research*, published online on 11
727 December 2015, DOI: 10.1080/00221686.2015.1116115.
728 Gong, J., Zecchin, A. C., Lambert, M. F., and Simpson, A. R. (2015b). "Study on the
729 frequency response function of viscoelastic pipelines using a multi-element
730 Kevin-Voigt model." *Procedia Engineering*, 119, 226–234.
731 Güney, M. S. (1983). "Waterhammer in viscoelastic pipes where cross-section parameters
732 are time dependent." BHRA Fluid Engineering, 189-204.
733 Keramat, A., Tijsseling, A. S., and Ahmadi, A. (2010). "Investigation of transient
734 cavitating flow in viscoelastic pipes." Institute of Physics Publishing.

825 Zecchin, A., Lambert, M., and Simpson, A. (2012). "Inverse laplace transform for
826 transient-state fluid line network simulation." *Journal of Engineering Mechanics*,
827 138(1), 101-115.
828 Zecchin, A. C., Simpson, A. R., and Lambert, M. F. (2008). "von Neumann stability
829 analysis of a method of characteristics visco-elastic pipeline model." *Proceedings*
830 *of the 10th International Conference on Pressure Surges*, BHR Group, Cranfield,
831 UK, 333-347.
832 Zhang, C., and Moore, I. D. (1997). "Nonlinear mechanical response of high density
833 polyethylene. Part I: experimental investigation and model evaluation." *Polymer*
834 *Engineering and Science*, 37(2), 404-413.
835 Zielke, W. (1968). "Frequency-dependent friction in transient pipe flow." *Journal of*
836 *Basic Engineering*, 90(1), 109-115.
837

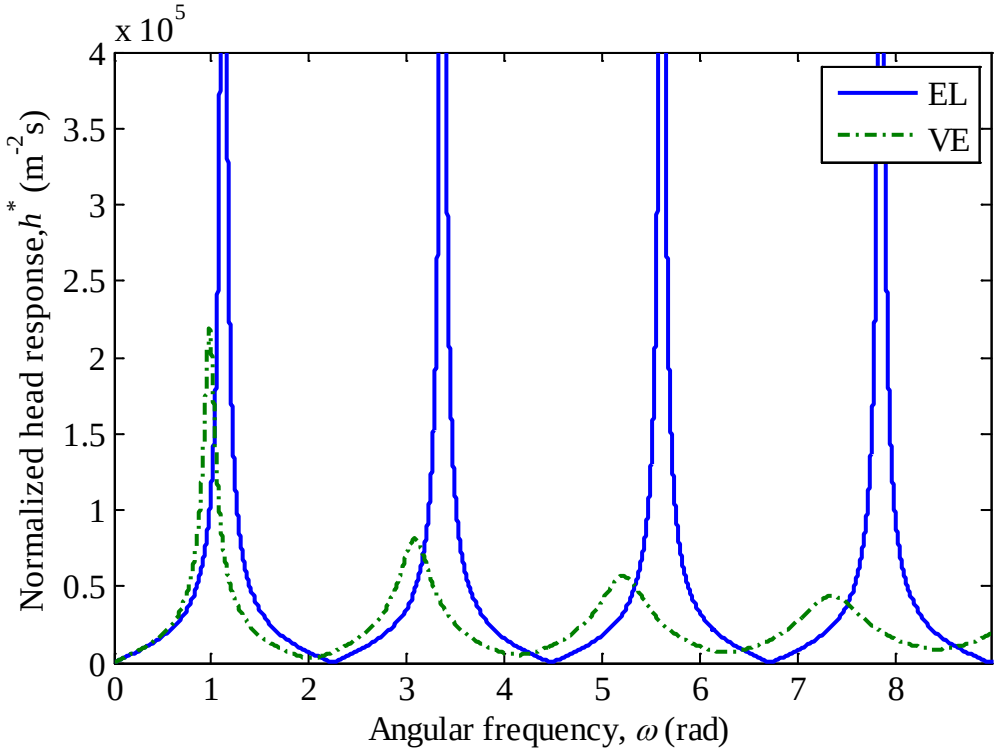


**Figure 3.** Theoretical FRDs of the reservoir-pipeline-closed valve system (case study 1) for the scenarios: (a) elastic and frictionless (EL, solid line) and (b) viscoelastic and frictionless (VE, dash-dotted line).

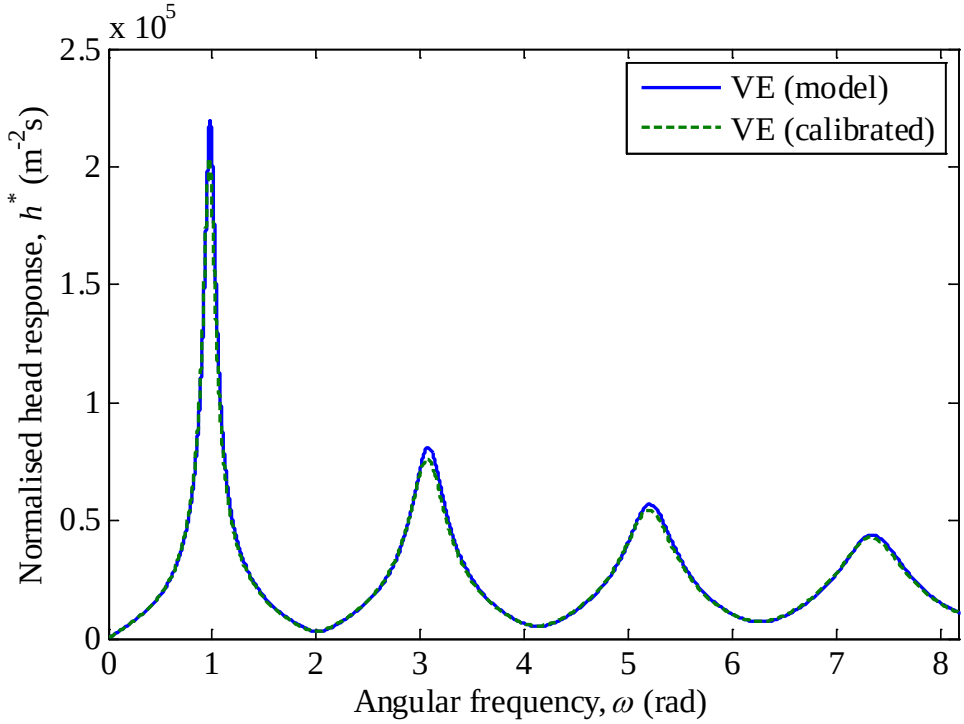


**Figure 4.** Comparison between the theoretical FRD (the solid line) and the calibrated FRD (the dashed line, using parameters calibrated in case study 1) for scenario VE of a reservoir-pipeline-closed valve system.

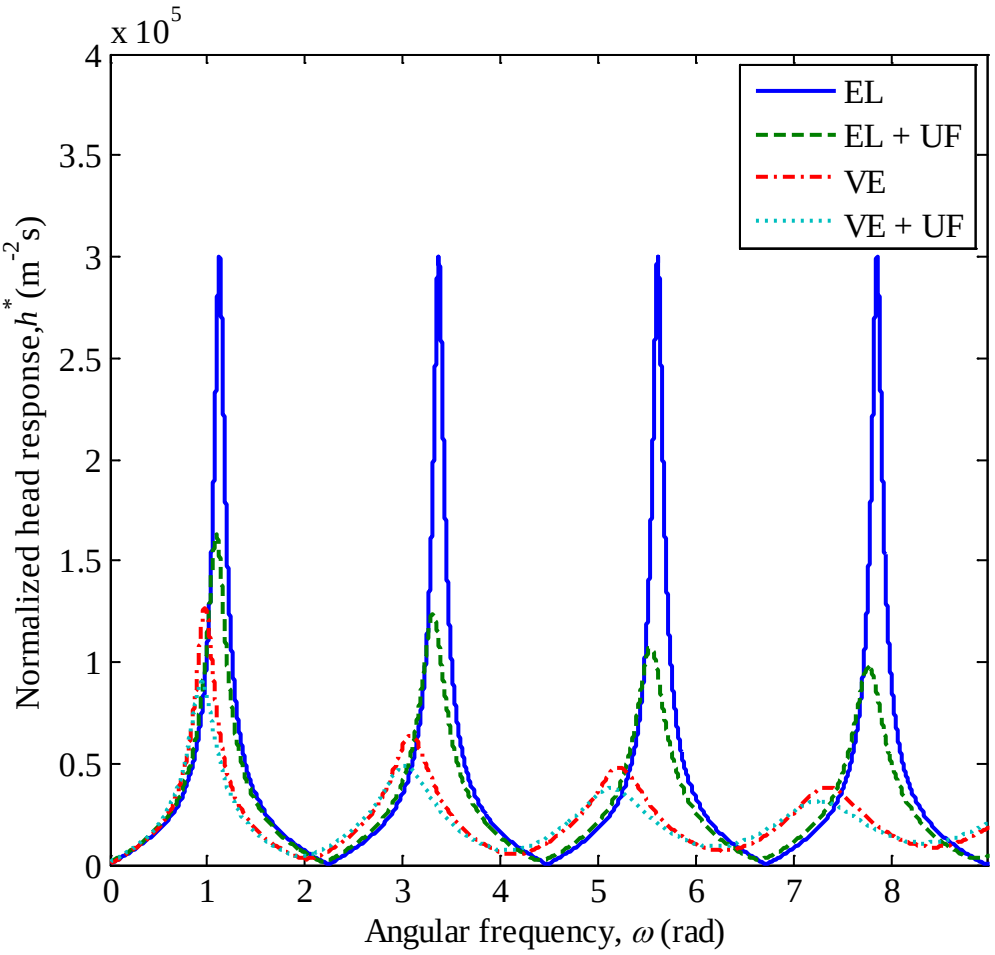


**Figure 5.** Theoretical FRDs for the scenarios: (a) elastic and frictionless (EL, solid line); (b) elastic with steady and unsteady friction (EL+UF, dashed line); (c) viscoelastic and frictionless (VE, dash-dotted line); and (d) viscoelastic with steady and unsteady friction (VE +UF, dotted line).

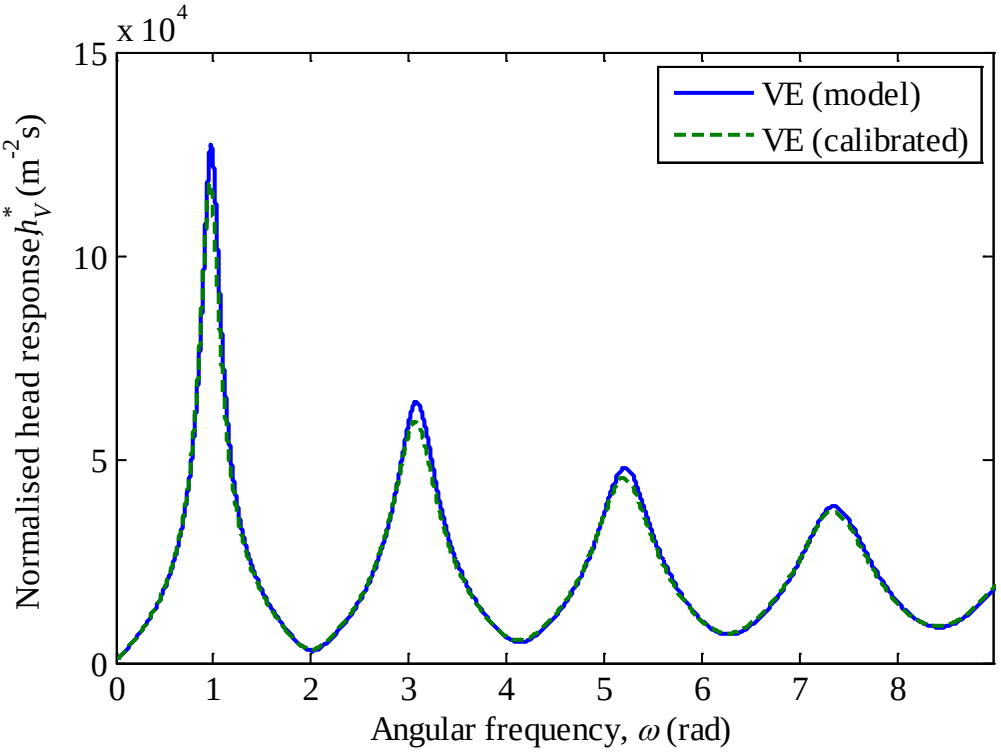


**Figure 6.** Comparison between the theoretical FRD (the solid line) and the calibrated FRD (the dashed line, use parameters calibrated in case study 2) for scenario VE of a reservoir-pipeline-high loss valve system.

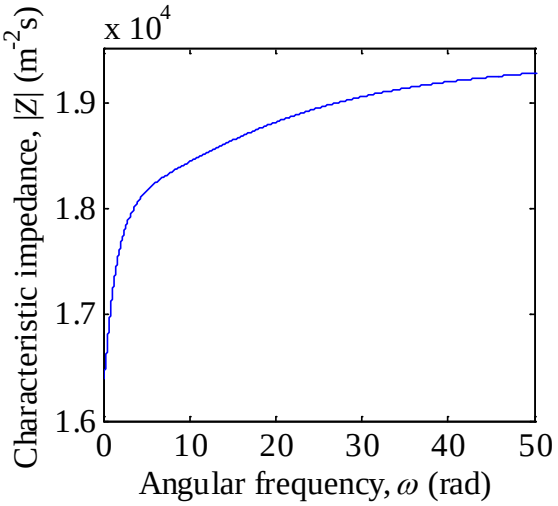


**Figure 7.** Absolute value of the characteristic impedance for the pipeline system in the *Case Studies*.

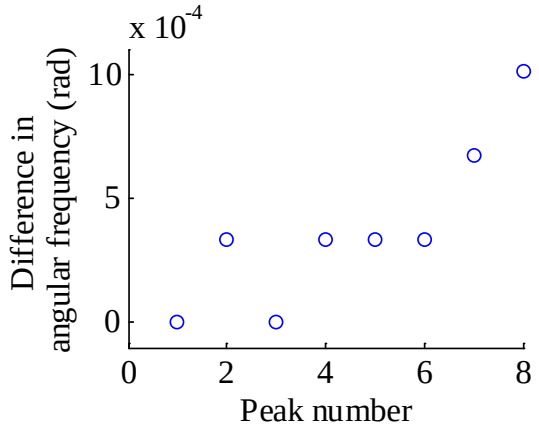


**Figure 8.** Difference in the peak frequencies between the functions $\left|Z\tanh(\mu L)\right|$ and $\left|\tanh(\mu L)\right|$ for the scenario viscoelastic and frictionless (VE) in the *Case Studies*.

**Tables**

**Table 1.** Specifications of the pipeline system used in the case studies

| Parameter | Value |
|---|---|
| Length $L$ (m) | 554 |
| Inner diameter $D$ (mm) | 50.6 |
| Wall thickness $e$ (mm) | 6.3 |
| Kinematic viscosity $\upsilon$ ($m^2/s$) | 1.004E−6 |
| Fluid density $\rho$ ($kg/m^3$) | 998.2 |
| Head of reservoir (m) | 45 |
| Steady-state flow rate (L/s) | 0.3 |
| Restraint coefficient $\alpha$ | 1.07 |
| Darcy-Weisbach friction factor $f$ | 0.02 |
| Reynolds number R | 7519 |
| Elastic wave speed $a_e$ (m/s) | 395 |

**Table 2.** Viscoelastic parameters used in the case studies

| Retardation time $\tau_k$ (s) | Compliance $J_k$ (10E−10 $Pa^{-1}$) |
|---|---|
| $\tau_1$ = 0.05 | $J_1$ = 1.044 |
| $\tau_2$ = 0.5 | $J_2$ = 1.037 |
| $\tau_3$ = 1.5 | $J_3$ = 1.145 |

**Table 3.** Theoretical resonant angular frequencies for the reservoir-pipeline-closed valve system under the scenarios: (a) elastic and frictionless (EL) and (b) viscoelastic and frictionless (VE).

| Peak number $m$ | Theoretical resonant frequency (rad) | |
|---|---|---|
| | EL | VE ( $\omega_m$ ) |
| 1 | 1.120 | 0.978 |
| 2 | 3.360 | 3.078 |
| 3 | 5.600 | 5.208 |
| 4 | 7.840 | 7.347 |

**Table 4.** Results of parameter evaluation using the resonant frequencies from the scenario viscoelastic and frictionless (VE) for *Case study 1*

| Parameter | Original model | Calibrated from VE | Relative error |
|---|---|---|---|
| $a_e$ (m/s) | 395 | 394.1 | -0.23% |
| $J_1$ (10E−10 $Pa^{-1}$) | 1.044 | 1.025 | -1.78% |
| $J_2$ (10E−10 $Pa^{-1}$) | 1.037 | 1.070 | 3.14% |
| $J_3$ (10E−10 $Pa^{-1}$) | 1.145 | 1.191 | 3.98% |

*Relative error = (Calibrated − Original)/ Original × 100%

**Table 5.** Theoretical resonant angular frequencies for the reservoir-pipeline-high loss valve system under the scenarios: (a) elastic and frictionless (EL); (b) elastic with steady and unsteady friction (EL+UF); (c) viscoelastic and frictionless (VE); and (d) viscoelastic with steady and unsteady friction (VE +UF).

| Peak number $m$ | Theoretical resonant frequency (rad) | | | |
|---|---|---|---|---|
| | EL | EL+UF | VE | VE+UF ( $\omega_m$ ) |
| 1 | 1.120 | 1.088 | 0.974 | 0.943 |
| 2 | 3.360 | 3.303 | 3.075 | 3.019 |
| 3 | 5.600 | 5.528 | 5.205 | 5.135 |
| 4 | 7.840 | 7.757 | 7.345 | 7.264 |

**Table 6.** Results of parameter evaluation using the resonant frequencies from the scenario viscoelastic with steady and unsteady friction (VE+UF) neglecting the effects of friction, for *Case study 2*.

| Parameter | Original model | Calibrated from VE+UF | Relative error |
|---|---|---|---|
| $a_e$ (m/s) | 395 | 396.9 | 0.49% |
| $J_1$ (10E−10 $Pa^{-1}$) | 1.044 | 1.314 | 25.83% |
| $J_2$ (10E−10 $Pa^{-1}$) | 1.037 | 1.473 | 42.05% |
| $J_3$ (10E−10 $Pa^{-1}$) | 1.145 | 1.736 | 51.64% |

*Relative error = (Calibrated − Original)/ Original × 100%

**Table 7.** Resonant angular frequencies calculated based on the elastic wave speed calibrated in the first attempt for the scenarios: (a) elastic and frictionless (EL); (b) elastic with steady and unsteady friction (EL+UF), and the estimated resonant angular frequencies for the scenario of viscoelastic and frictionless (VE).

| Peak number $m$ | Calculated resonant frequency (rad) | | |
|---|---|---|---|
| | EL ($\omega_{m\_FL}$) | EL+UF ($\omega_{m\_UF}$) | VE approx. ($\omega_{m\_C}$) |
| 1 | 1.125 | 1.093 | 0.971 |
| 2 | 3.376 | 3.318 | 3.072 |
| 3 | 5.627 | 5.554 | 5.203 |
| 4 | 7.878 | 7.794 | 7.342 |

**Table 8.** Results of parameter evaluation using the resonant frequency approximations for scenario viscoelastic and frictionless (VE), for *Case study 2*.

| Parameter | Original model | Calibrated from VE approx. | Relative error |
|---|---|---|---|
| $a_e$ (m/s) | 395 | 393.1 | -0.49% |
| $J_1$ (10E−10 $Pa^{-1}$) | 1.044 | 0.983 | -5.88% |
| $J_2$ (10E−10 $Pa^{-1}$) | 1.037 | 1.158 | 11.64% |
| $J_3$ (10E−10 $Pa^{-1}$) | 1.145 | 1.373 | 19.89% |

*Relative error = (Calibrated − Original)/ Original × 100%

**Table 9.** Results of parameter evaluation for the modified pipeline system with a length of 277 m (half of that used in the previous *Case Studies*)

| Parameter | Original model | Calibrated with $\tau_1$ = 0.05 s, $\tau_2$ = 0.5 s, $\tau_3$ = 1.5 s | Relative error | Calibrated with $\tau_1$ = 0.05 s, $\tau_2$ = 0.25 s, $\tau_3$ = 1.0 s | Relative error |
|---|---|---|---|---|---|
| $a_e$ (m/s) | 395 | 395.1 | 0.03% | 395.3 | 0.07% |
| $J_1$ (10E−10 $Pa^{-1}$) | 1.044 | 1.086 | 3.98% | 1.097 | 5.07% |
| $J_2$ (10E−10 $Pa^{-1}$) | 1.037 | 7.261 | -29.98% | 1.043 | 0.62% |
| $J_3$ (10E−10 $Pa^{-1}$) | 1.145 | 2.598 | 126.88% | 1.190 | 3.92% |

*Relative error = (Calibrated − Original)/ Original × 100%